INVESTIGATION OF DROPLET COLLISIONS OF VISCOUS PROCESS FLUIDS BY IMAGING TECHNIQUES

Stefan Blei*, Martin Sommerfeld*

* Department of Engineering Science, Martin Luther Universität Halle-Wittenberg,
06099 Halle, Germany
phone: +49-3461-462836 fax: +49-3461-462878
email: Stefan.Blei@iw.uni-halle.de

ABSTRACT

Knowledge about the outcome of collisions between droplets in sprays is essential for predicting drop size distributions. In the frame of this work collisions of droplets are investigated which fluid is a composition of proteins, fat globules, different carbohydrates and water as solvent and hence higher viscous. This composition prevents the application of measurement techniques such as Phase Doppler anemometry. For that reason an image based measurement system is developed enabling the measurement of relevant data such as droplet diameters and shape, velocity and other information. The non-Newtonian viscosity of the droplet fluid prevents a regular droplet breakup by the Rayleigh-mechanism. Hence, an algorithm is introduced giving access to the individual parameters of the occurring droplet collisions. The quality of the method is demonstrated by an error analysis and the effect onto the accuracy for the determination of the impact parameter and the Weber number is discussed. Exemplary, experimental results are shown for one of three used product. This soy based milk product has a non-Newtonian viscosity. The gained boundary between coalescence and stretching separation agrees with data obtained for a Newtonian fluid by Havelka et al. (2004).

INTRODUCTION

During a number of industrial processes, especially spray drying processes, dispersed phase interaction occurs in which droplets are involved consisting of liquid being suspension, emulsion and solution. Such droplets usually have fluid properties significantly different from that of water. For example the viscosity value of milk products during spray drying is at the initial stage (just after atomisation) between 10 and 300 mPa s, and during the drying process this value raises to $10^6 – 10^8$ Pa·s before the droplets are considered to be dry due to glass transition. Especially these high viscosity values lead to different collision outcomes compared to that of water or Alkanes. Only little knowledge is available even for liquids at the initial stage directly after atomisation, despite collisions between viscous droplets can be followed by agglomerate build up. Orme (1997) summarized the information available for water and non-water droplet collisions. The degree of agglomeration, and even more, the structure and composition of agglomerates are enormously important for product properties as powder-solubility or powder porosity.

Hence, investigations of the collision behaviour of higher viscous droplets in the micrometer range (spray dried milk droplets usually have sizes between 20 and 80µm) are strongly desirable. Since the investigated fluids (milk products) are simultaneously suspension, emulsion and solution (they include fat, crystals, soluble proteins and other components), the droplets do not have homogeneous optical properties (Menn et al. 2003). This prevents the application of Phase-Doppler Anemometry for the measurement of size and velocity distributions. Imaging techniques are much more promising.

AIM OF THE INVESTIGATION

The present work is focused on the investigation of the collision behaviour of different types of milk products as processed in the food industry by spray drying. The investigated products have dynamic viscosity values in the range of 16 to 200 mPa s (shear thinning liquid) and a surface tension of around 42 mN/m. The boundaries between separation and coalescence of colliding droplets of different size and drying state were of special interest of the investigation. Additionally, individual impact parameters of colliding droplets and their size and velocity should be measured. In order to enable such a detailed measurement, a new imaging based measurement procedure was developed.

EXPERIMENTAL SETUP AND MEASUREMENT TECHNIQUE

The experimental setup can be distinguished in the droplet generation system and the image based measurement system.

Droplet generation system

Two droplet chains were created using two membrane nozzles. The core of the droplet generation system are two nozzles delivered by Inotech Encapsulation (Dottikon, Switzerland). Originally used for encapsulation purposes, the nozzles consist of an electrical coil, a Teflon membrane on which a magnet is fixed, a pulsation chamber and an orifice for the liquid outlet (Fig. 1). The membranes were excited by a magnetic field, set up by the coil, with a sinusoidal oscillation. That supports a regular Rayleigh-breakup of the liquid being pressed through the nozzle, as described for example by König et al. (1986). A heatabel vessel contained the liquid which was forced to flow to the nozzle by pressurized air. The air pressure itself was regulated by a fine tunable pressure valve and was in the range between 0.2 and 2 bar.

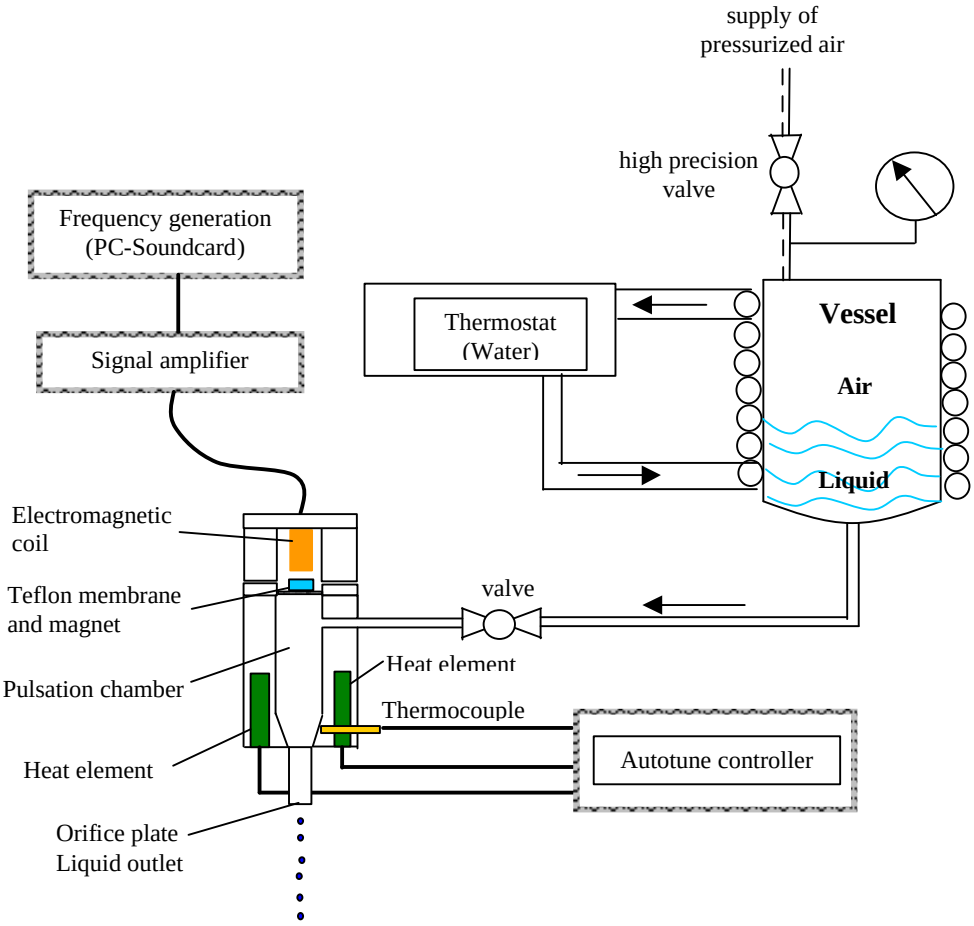

Fig. 1: Schematic view of the liquid supply system and the droplet generator.

The excitation works reasonably well for Newtonian liquids, but showed almost no impact on the breakup of non-Newtonian liquids as some of the investigated milk products which had to be heated up to 75°C (process condition). Hence, a random breakup of droplets occurred leading to a variation of droplet size and velocity inside a droplet chain. Impacts between droplets of the two jets (Fig. 4) became stochastic events with stochastic collision arrangements.

Measurement System

Despite the characteristics of stochastic droplet breakup a detailed measurement of impact parameter and Weber number should be enabled. Hence, the evaluation of individual droplet impacts became necessary. So an image based measurement technique was applied extended with newly developed evaluation routines for the image processing.

The measurement system consists of a Nd-YAG double pulse laser and a CCD-camera to take pairs of images with short time delay (~15µs), enabling the application of a PTV-algorithm for the velocity determination. A second camera system is used to align the droplet streams forcing collisions and to judge collision phenomena in the plane perpendicular to the plane of measurement (Fig. 2). A lense system, a Rhodamin-B solution and an opal plate were used to weaken the Gaussian light intensity profile of the laser beam and to widen the illuminated area. Macro lenses with defined depth of field were mounted on the cameras enabling a precise determination of sizes and distances across the entire chip size of 1284 x 1024 pixles. The usage of frequency generators ensured a proper control of exposure times which is important to minimize failures of the velocity determination.

Image evaluation technique

With help of an extended and partly newly developed image processing software the pairs of images were evaluated. Due to the availability of fast computers and the use of timer cards a full online-measurement and image evaluation could be achieved at

a rate of 4 double-frames per second (the limit is the read-out time of the camera chip). But because of the complexity of the task the images were still stored on hard-disc to keep further access. By applying a gradient based segmentation method the droplet objects were separated from the image background (Bröder 2004, Fig. 3 and 4). Diameters, 2D-velocity vectors, the position within the image and shape factors were calculated.

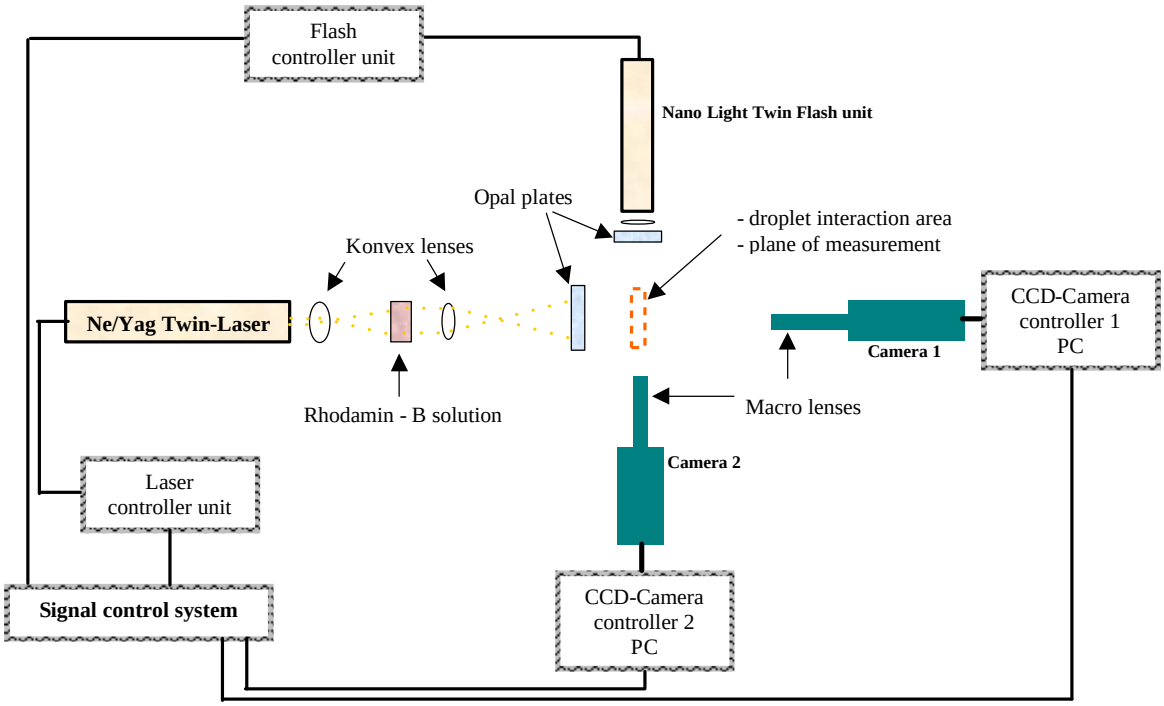

Fig. 2: Image based measurement system as used during the experiments.

In order to estimate the impact parameters and other properties, the droplets captured on the image were tracked in the frame of the images, using the initial location in the image, the droplet size and the velocity vector of each droplet. During this tracking the droplet velocity was assumed to be constant. The tracking was terminated as soon as the droplets touched the surface of another tracked droplet. This yields the impact geometry wherefrom the following parameters were estimated: collision partner, diameters of partners, impact parameter, relative collision velocity, Weber number and location of the collision in the image.

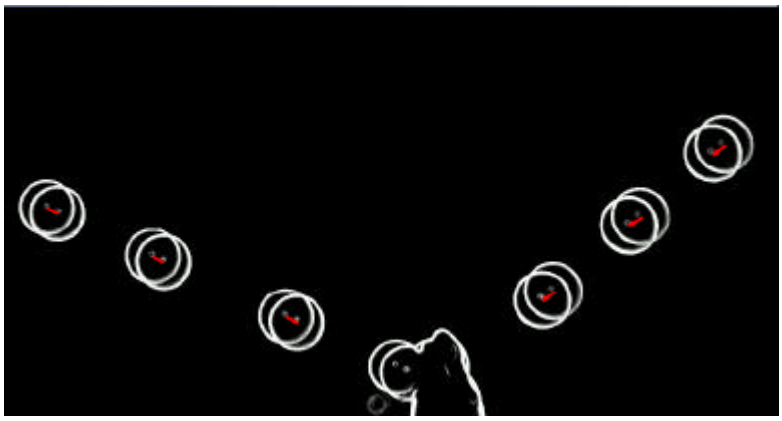

Fig. 3:
Image evaluation by a gradient based segmentation method and a PTV algorithm. In the picture the edges of the droplets as detected by the gradient filter are shown. The contours of the droplets on two successive images are drawn in one picture, with the velocity vector between the centres of both.

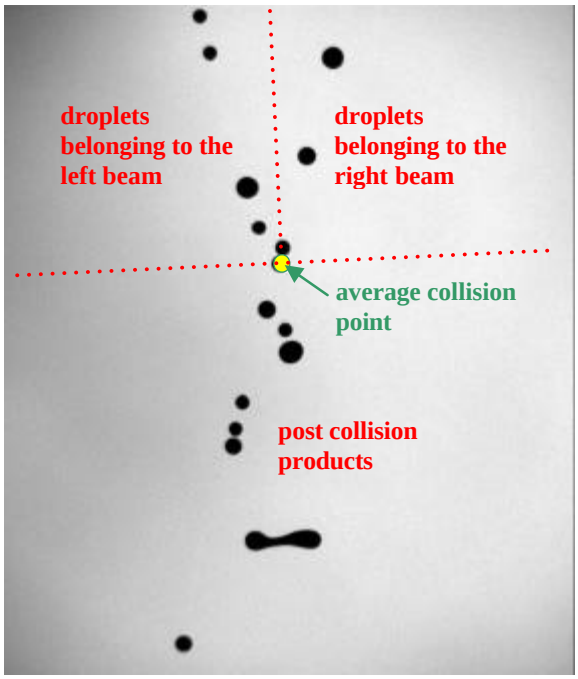

Fig. 4:
Configuration for the statistical evaluation of the images showing droplet impacts.

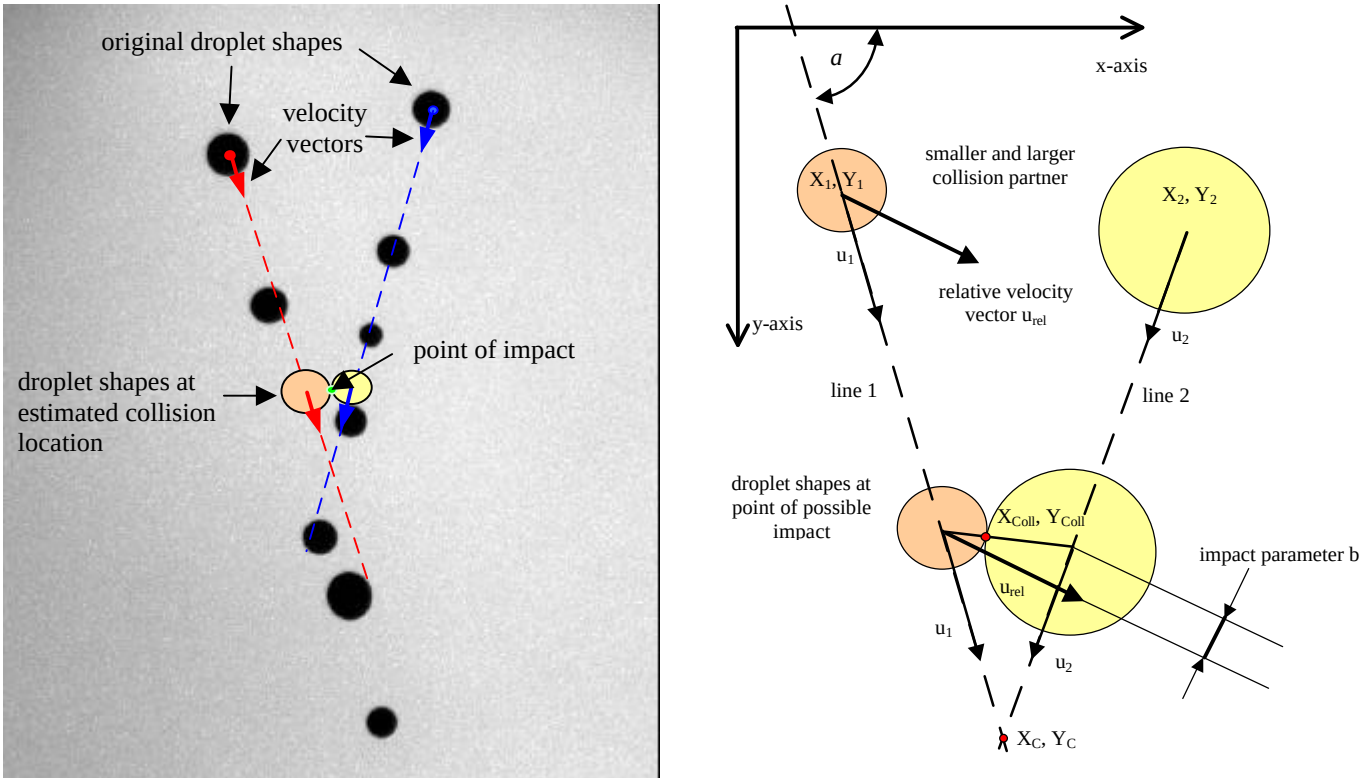

Fig. 5: Tracking of droplet shapes in the images and estimation of the impact parameter and relative velocity vector

The location of collision was further used to distinguish between pre- and post collision droplets. Averaging all detected collision points, the droplets were ordered to belong to the left or right droplet chain or to belong to the collision products. The occurrence of collision phenomena, such as, coalescence, stretching separation or splashing were still determined manually by viewing the images. In order to characterise an individual collision event of the stochastically colliding droplet pairs, a temporal resolution of the collision process would be necessary. This could not be realised in the frame of the present investigation, since the maximum frequency for double images was limited to 4 Hz.

Accuracy of parameter estimation

According to Bröder (2004) the error of determining the centre of gravity (COG) of an image object with the described edge detection algorithm is around 0.1 Pixel both in x and y direction. The error included by the time shift between the two images used for the velocity calculation is seen to be smaller than 0.1 µs, independent of the value of the time shift. The geometrical error leads to a shift of the direction of the velocity vector, and the timing error to a variation of the length of the velocity vector. This error is extrapolated by applying the described image evaluation method and effects the accuracy of determining the collision point and the impact parameter (Fig. 6). Fig. 6 shows the importance of the object size in the image. As smaller the object as bigger is the negative influence of the Centre-of-Gravity-error onto the exactness of the impact parameter measurements. The value of the collision angle is of minor importance. The geometrical length of the velocity vector has to exceed at least 30% of the object diameter to avoid unacceptable errors.

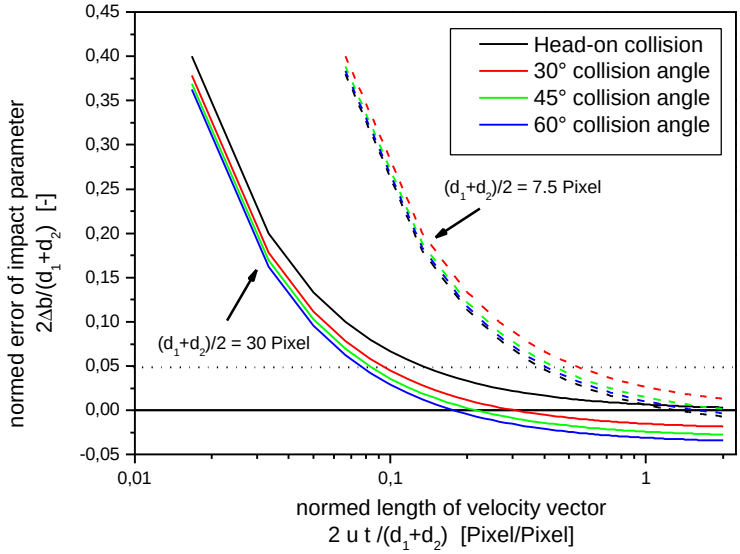

Fig. 6:

Normealized error of the impact parameter caused by the exactness of the COG-determintaion. This error is reduced with increasing geometrical length of the velocity vector and with increasing object size.

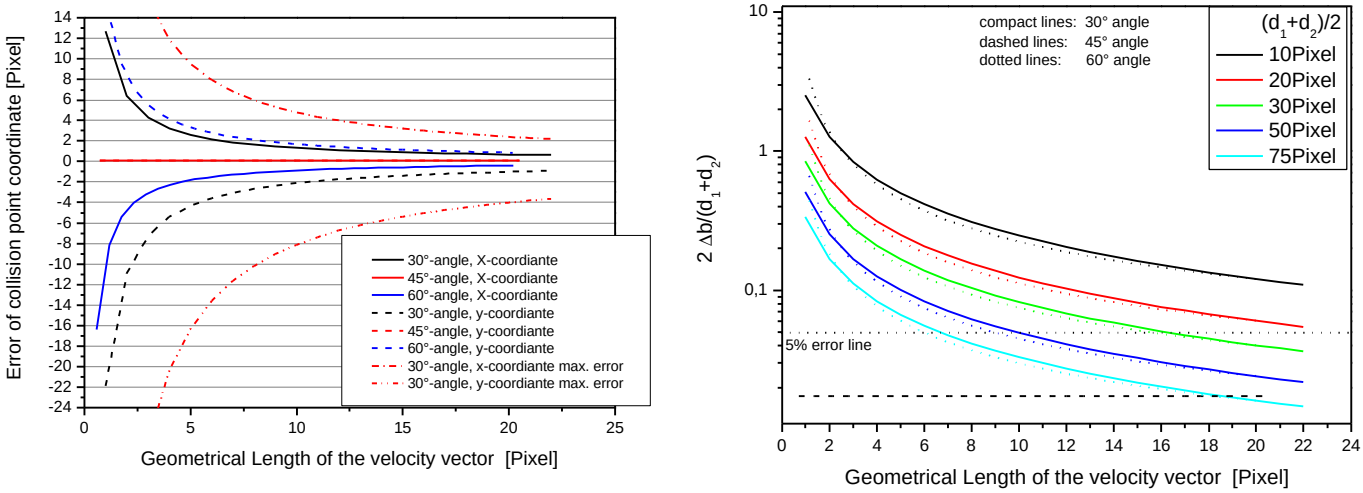

Fig. 7: Error made during the collision point determination (left) and it's effect onto the impact parameter (right)

As shown in Fig. 7 (left), the errors made during the determination of the centres-of-gravity are not neglegtable. To reduce the error below 2 Pixel, the velocity vector should have a minimum length of at least 10 Pixels. But even that will not prevent inacceptable errors in worst-case scenarios.

The influence of the error of the collision point determination onto the calculation of the impact parameter is significant (Fig. 7, right). A relatively large object size reduces the error, so acceptable error values can be achieved. The collision angle has only a minor influence on the error value.

RESULTS AND DISCUSSION

Experiments were carried out for 3 different product liquids which are typically used in the spray drying industry. These products contain dissolved and suspended ingredients which change their material properties during the drying process. In order to capture the change of material properties the content of solvent (water) was varied. Two of the products (a soy based and whey based milk product) were non-Newtonian with zero-shear viscosity values between 2 and 300 mPa·s and a surface tension of around 0.044 N/m. The third product, a whey permeate concentrate, showed an almost Newtonian viscosity behaviour with μ=95 mPa s and a surface tension of 0.0418 N/m.

The stochastic droplet breakup and the discussed errors of the PTV algorithm lead to a wide distribution of impact parameters (Fig. 8). This fact prevented the creation of a detailed chart of the impact parameter as function of the Weber number as proposed for example by Brenn (2001). Hence, the evaluation of the experiments was concentrated onto the determination of dominating collision regimes (i.e. coalescence and stretching separation) and the statistical description of the observed droplet population before and after the collision events. The gained individual droplet information was sorted to belong either to the left or right droplet chain (before collision) or to the collision products (after collision) (Fig. 4). Within these three groups distributions of mean- and standard deviation values of the droplet size, velocity, sphericity and other properties were calculated.

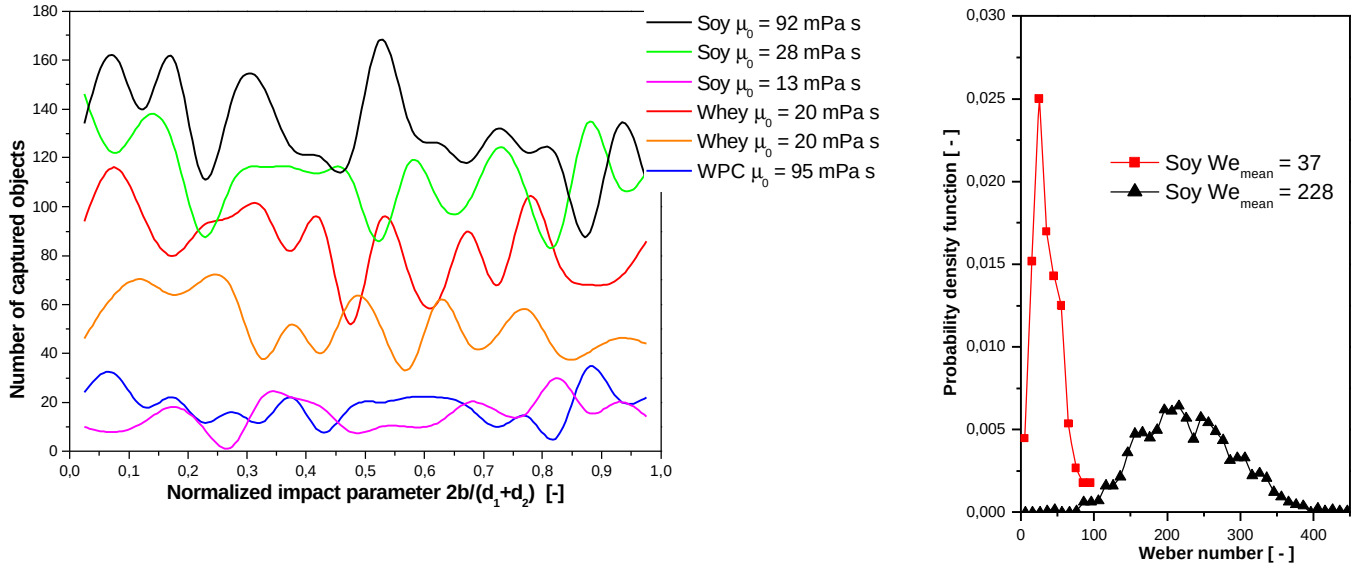

Fig. 8: Distribution of the impact parameters (left) for different products and different measurement series showing their random occurance. On the right the probability density function of impact Weber numbers is shown for a low and a high Weber number serie of the soy product.

Despite the problem of wide distributions of Weber numbers and impact parameters within all series of measurement, mean values of the impact parameter and the Weber number are used to compare the experimental results of the soy based product with data obtained by Havelka et al. (2004) for a Newtonian liquid (TEG - tri-ethylene-glycol) (Fig. 9). The TEG-fluid has very similar density, zero-shear viscosity and surface tension values compared to the soy and whey based products and therefore it is suitable for comparison purposes. Due to the described measurement difficulties no bouncing regime could be observed for the soy base product. The points for coalescence and stretching separation agree well and lay within the boundaries between coalescence and stretching separation of the TEG-fluid. The higher viscous soy droplets (μ_0 = 90 mPa s) coalesce at higher Weber numbers than the TEG droplets. In general, for increasing viscosity values a tendential shift of the critical Weber number (boundary coalescence – stretching separation) towards higher Weber numbers could clearly be observed (Fig. 9). This finding agrees with results of Jiang et al. (1992).

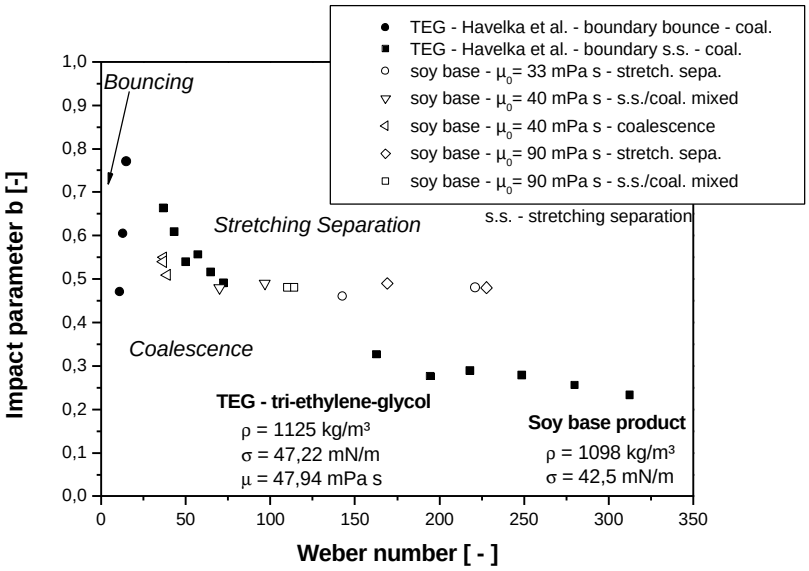

Fig. 9:

Comparison of results for the non-Newtonian liquid soy base and data of a Newtonian liquid (TEG) obtained by Havelka et al. (2004). All data points of soy base are mean values of the impact parameter and the Weber number describing the dominating collision phenomena of the measurement serie. These data points represent a distribution of impact parameters and Weber numbers as shown in Fig. 8. μ_0 is the estimated zero-shear viscosity value.

CONCLUSIONS

The investigation of drop-drop-collisions in which the droplets consist of higher viscous, non-Newtonian liquids being suspension, emulsion and solution at once is still a challenging task. Droplet breakup from laminar jets is usually a stochastic event preventing the utilization of established measurement methods (König 1986, Brenn 2001). Hence, an image based method was developed to determine pre-collision conditions of the droplets as well as data for the post collision fluid objects. A new tracking algorithm was developed to gain information about the impact parameter and Weber number of individual droplet pairs in a stochastic droplet chain. An extensive error analysis revealed the applicability of the developed method. Despite the difficulties faced due to irregular droplet breakup for non-Newtonian liquids the boundaries between coalescence and separation agree with that found by Havelka et al. (2004) for a Newtonian liquid with nearly similar material properties. A shift of the critical Weber number towards higher values for increasing fluid viscosity is observed as well, in agreement with literature (Jiang et al. 1992).

The authors would gratefully acknowledge the support of the present work by the EC Fifth Framework Programme "Growth", contract number G1RD-CT-2000-00340, and all partners involved in the "EDECAD"-project („**E**fficient **DE**sign and **C**ontrol of **A**gglomeration in spray **D**rying machines - '**EDECAD**' " , www.EDECAD.com).

REFERENCES

1. G. Brenn, D. Valkovska, K.D. Danov: The formation of satellite droplets by unstable binary drop collisions. Physics of Fluids Vol. 13, no. 9, pp. 2463-2477, 2001.
2. D. Bröder: Anwendung optischer Messtechniken zur Untersuchung disperser Gas-Flüssigkeits-Strömungen. Dissertation. Halle (Saale) 2004.
3. P. Havelka, C. Gotaas, H. A. Jakobsen, H.F. Svendsen: Droplet formation and Interactions under normal and high pressure. Proceedings 5th International Conference on Multiphase Flow ICMF '04, Yokohama/Japan, 2004, paper no. 123.
4. Y. J. Jiang, A. Umemura, C. K. Law: An experimental investigation on the collision behavior of hydrocarbon droplets. J. Fluid Mech. 234, pp. 171-190, 1992.
5. G. König, K. Anders, A. Frohn: A new light-scattering technique to measure the diameter of periodically generated moving droplets. J. aerosol Science, Vol. 17, No. 2, pp. 157-167, 1986.
6. P. Menn, G. Schulte, K. Bauckhage: Experimental investigation of high pressure spray drying nozzle performance at industrial operating conditions. ICLASS 2003 Sorrento/Italy, paper no. 1602.
7. Orme M. (1997) Experiments on droplet collision, bounce, coalescence and disruption. Progress in Energy and Combustion Science vol. 23, pp. 65-79.